Journal of Molecular Structure 1372 (2026) 146580

Contents lists available at ScienceDirect

Journal of Molecular Structure

journal homepage: www.elsevier.com/locate/molstr

Antioxidant capacity and α-glucosidase inhibitor activity of *Bryonia aspera* extracts and its major constituent p-coumaric acid: Phytochemical analysis, biological evaluation and computational approach

Salih Tuncay [a,b,*], Ömer Faruk Karasakal [c], Mikail Açar [d], İsra Toptancı [e], Halil Şenol [f], Olgun Çırak [g], Mesut Işık [h], Şükrü Beydemir [i]

[a] Üsküdar University, Vocational School of Health Sciences, Department of Food Technology, 34662, Istanbul, Türkiye
[b] Atabay Pharmaceuticals and Fine Chemicals Inc, Acıbadem R&D center, 34718, Kadıköy Istanbul, Türkiye
[c] Department of Medical Laboratory, Vocational School of Health Services, Uskudar University, Türkiye
[d] Munzur University, Tunceli Vocational School of Higher Education, Department of Plant and Animal Production, Tunceli, Türkiye
[e] Istanbul Food Control Laboratory, Istanbul, Türkiye
[f] Faculty of Pharmacy, Department of Pharmaceutical Chemistry, Bezmialem Vakif University, Fatih, Istanbul, 34093, Türkiye
[g] Department of Hospitality Restaurant and Catering Services, Vocational School, Bilecik Şeyh Edebali University, Bilecik, Türkiye
[h] Department of Bioengineering, Faculty of Engineering, Bilecik Şeyh Edebali University, Bilecik, Türkiye
[i] Department of Biochemistry, Faculty of Pharmacy, Anadolu University, Eskişehir, Türkiye

ARTICLE INFO

Keywords:
Cucurbitaceae
B. aspera
P-coumaric acid
Antioxidant activity
α-glucosidase inhibition
Molecular docking

ABSTRACT

This study comprehensively investigated the phenolic composition, antioxidant potential, and α-glucosidase inhibitory properties of *B. aspera* Steven ex Ledeb. extracts using integrated *in vitro* and *in silico* approaches. LC-MS/MS analysis identified seven major phenolic compounds, caffeic acid, chlorogenic acid, galangin, gallic acid, naringenin, p-coumaric acid, and rutin, with p-coumaric acid being the most abundant (306.71 mg/kg in aerial and 155.56 mg/kg in root extracts). Both extracts exhibited strong antioxidant and α-glucosidase inhibitory activities, particularly the aerial extract (IC_{50} = 0.678 and 0.173 for DPPH, ABTS, respectively and 0.022 mg/mL for α-glucosidase inhibition). Molecular docking and MM-GBSA analyses supported these findings, showing that p-coumaric acid had the strongest binding to α-glucosidase (–7.783 kcal/mol, ΔG = –47.76 kcal/mol), stabilized by key interactions with Asp-62, Arg-200, His-332, and Arg-400. A 250 ns molecular dynamics simulation confirmed the stability of the complex, and *in silico* ADME analysis revealed good oral absorption (67%) and compliance with Lipinski's rule. Overall, results indicate that p-coumaric acid is the primary bioactive compound contributing to the antioxidant and α-glucosidase inhibitory activity of *B. aspera*, with promising potential as a natural lead for α-glucosidase inhibition.

1. Introduction

Nature provides a wide variety of plants known for their therapeutic properties in treating a variety of ailments. Due to their low toxicity and cost-effectiveness, medicinal plants have been used by numerous cultures throughout history to treat a variety of ailments [1–5]. This enduring tradition has generated significant interest in the development of herbal medicines, often linked to the presence of phytochemicals. According to data from the World Health Organization (WHO), approximately 80% of the global population relies primarily on medicinal plants for basic healthcare needs [6]. In recent years, there has been an increasing focus on investigating the therapeutic potential of natural plant-based antioxidants, whether in the form of crude extracts or incorporated into functional foods [7,8]. The bioactive components present in the extracts exhibit synergistic interactions that are believed to be beneficial in addressing chronic, multifaceted disorders involving various pathways [9–11].

Diabetes is a chronic and debilitating disease characterized by a series of events that lead to decreased or inhibited insulin secretion from the pancreas. When insulin production or utilization is inadequate, it leads to hyperglycemia, resulting in high blood sugar levels and, over time, damage to organs and tissues [12,13]. Currently,

* Corresponding author.
E-mail address: salih.tuncay@uskudar.edu.tr (S. Tuncay).

https://doi.org/10.1016/j.molstruc.2026.146580
Received 27 November 2025; Received in revised form 2 May 2026; Accepted 16 May 2026
Available online 19 May 2026

antihyperglycemic agents such as acarbose, voglibose, and miglitol are available to prevent postprandial hyperglycemia [14–17]. Current medications may be effective in reducing hyperglycemia in diabetic patients. However, long-term use is associated with side effects such as liver toxicity, abdominal bloating, gas, and increased frequency of diarrhea [18]. The plant *Bryonia aspera* belongs to the Cucurbitaceae family and contains many kinds of cucurbitacins. The *Bryonia* genus is represented by 10 species in the worldwide and 5 species in Turkey. The Turkish name of *Bryonia aspera* is Şeytanşalgamı, but it is also known by various local names in the regions where it is distributed (such as 'rehe abdülselam', 'tilkikuyruğu', 'Xezirvik'). Cucurbit plants are widely utilized as traditional herbal medicines for a variety of diseases because they have shown anti-inflammatory [19,20], anti-tumor, hepatoprotective [21], and immunomodulatory properties [22].

The biological activities of the genus *Bryonia* were uncovered by a thorough investigation. These activities included intriguing anticancer activity in addition to antioxidant, antidiabetic [23], antibacterial [24, 25], antinociceptive [23], and anti-inflammatory properties [26–28]. Antioxidant activity studies on the *B. aspera* plant show that it protects against oxidative stress. At the same time, in a study that shows it has hypoglycemic properties in particular, an ethanolic extract of *B. aspera* significantly reduced blood glucose levels in streptozotocin-induced diabetic rats, thus indicating that it may be effective against hyperglycemia [29–33]. *B. aspera*, which has been reported in the literature to have various biological activities, is considered a potential natural drug source in modern medicine. For example, an ethnopharmacological study in the literature reported that Iranians used the *B. aspera* plant to treat cancer, digestive problems, and liver disorders [34]. In addition to its diverse traditional uses worldwide, *B. aspera* has also been reported to be used in the treatment of diabetes in Türkiye [35]. Our ethnobotanical field studies further revealed its use in the treatment of headache, toothache, diabetes, and fever, as well as its consumption as a food source.

The aim of this study was to comprehensively investigate the phytochemical profile and biological activities of *B. aspera*. For this purpose, extracts obtained separately from the aerial and root parts were analyzed by LC-MS/MS to identify their phenolic, flavonoid, and organic acid compositions. Furthermore, their antioxidant and α-glucosidase inhibitory activities were evaluated and compared with reference controls. To gain further mechanistic insights, molecular docking and dynamics studies were performed to explore the potential interactions of the major identified compounds with α-glucosidase and other relevant targets. In the present study, the aerial (AP) and root (RP) parts of *B. aspera* were found to contain the highest levels of *p*-coumaric acid among the detected phenolic and flavonoid compounds, with concentrations of 294.74 mg/kg (AP) and 149.69 mg/kg (RP), respectively.

2. Results and discussion

2.1. Phenolic composition

The aerial and root parts of *B. aspera* were extracted separately, and the obtained extracts were analyzed by LC-MS/MS [36]. A total of eighteen reference standards including catechin, naringenin, gallic acid, caffeic acid, chlorogenic acid, *p*-coumaric acid, hesperidin, rutin, oleuropein, myricetin, quercetin, kaempferol, genistein, apigenin, pinocembrin, caffeic acid phenethyl ester, chrysin, and galangin were employed to identify phenolic, flavonoid, and organic acid constituents in the extracts [37,38]. The analysis indicated that seven compounds which are **caffeic acid, chlorogenic acid, galangin, gallic acid, naringenin, *p*-coumaric acid** and **rutin** were detected as the major constituents, with ***p*-coumaric acid** being particularly abundant in both aerial and root extracts (Table 1).

LC-MS/MS analysis of *B. aspera* revealed the presence of seven major phenolic and flavonoid compounds in both aerial part and root extracts. Among these, ***p*-coumaric acid** was identified as the predominant constituent in both extracts, reaching remarkably high levels in the aerial part extract (306.71 mg/kg) compared to the root extract (155.56 mg/kg). This suggests that p-coumaric acid is the key phenolic marker of the species and may play a major role in its biological activities .

Table 1
Phenolic compounds detected in black and root extracts *(two replicates)* of *Byrona aspera*.

Compounds	Aerial Part Extract (mg/kg)	Root Extract (mg/kg)
Caffeic acid	16.01	2.53
Chlorogenic acid	11.36	–
Galangin	0.37	–
Gallic acid	20.43	1.85
Naringenin	0.92	0.47
***p*-Coumaric acid**	**306.71**	**155.56**
Rutin	8.08	–

Other phenolic acids such as caffeic acid and gallic acid were also present in both extracts, but at considerably higher concentrations in the aerial part extract (caffeic acid: 16 mg/kg; gallic acid: 20.4 mg/kg) than in the root extract (caffeic acid: 2.5 mg/kg; gallic acid: 1.8 mg/kg). Similarly, naringenin was detected in both extracts, with levels approximately two-fold higher in the aerial part extract compared to the root extract. Certain compounds, chlorogenic acid, galangin, and rutin, were exclusively detected in the aerial part extract, while being absent in the root extract. This qualitative difference indicates that the aerial part extract possesses a broader and more diverse phenolic profile. The presence of ***p*-coumaric acid** as the major phenolic constituent in both aerial and root extracts was further confirmed by LC-MS/MS analysis, which showed sharp peaks at retention times of 3.61 min (aerial extract) and 3.60 min (root extract) (Fig. 1).

2.2. Antioxidant capacity and α-glucosidase inhibitory activity

The antioxidant activity of *B. aspera* extracts and p-coumaric acid were evaluated using two widely applied *in vitro* assays, namely DPPH and ABTS radical scavenging tests, which provide complementary information on the free radical scavenging ability of plant-derived compounds. In addition, their α-glucosidase inhibitory potential was assessed through an α-glucosidase inhibition assay, a standard *in vitro* method for evaluating the ability of natural products to modulate carbohydrate metabolism. In all assays, biological activity was quantified based on IC_{50} values, where a lower IC_{50} indicates stronger radical scavenging or enzyme inhibitory efficiency. The antioxidant capacity (DPPH and ABTS) and α-glucosidase inhibitory activity of *B. aspera* extracts as well as p-coumaric acid are summarized in Table 2.

As shown in Table 2, both aerial and root extracts of *B. aspera* exhibited measurable antioxidant capacity. In the DPPH assay, the aerial part demonstrated stronger radical scavenging activity (IC_{50} = 0.678 mg/mL, R^2 = 0.997) compared to the root extract (IC_{50} = 3.877 mg/mL, R^2 = 0.954). In the ABTS assay, both extracts showed higher potency, with IC_{50} values of 0.173 mg/mL (aerial, R^2 = 0.969) and 0.457 mg/mL (root, R^2 = 0.948).Among the detected compounds, p-coumaric acid, which is most abundant compound in both extracts, exhibited substantial antioxidant capacity (IC_{50} = 0.563 mg/mL for DPPH, R^2 = 0.985 and 0.0003 mg/mL for ABTS, R^2 = 0.997), confirming its contribution to the overall activity of the extracts.

Although the positive control trolox displayed far superior activity (IC_{50} = 0.006 mg/mL for DPPH and 0.003 mg/mL for ABTS), both extracts demonstrated notable radical scavenging potential.Overall, the aerial extract was consistently more active than the root extract, indicating that antioxidant constituents such as *p*-coumaric acid are likely more abundant in aerial tissues. In a previous study, the antioxidant potential of various parts of Cucurbitaceae vegetables was investigated. ABTS radical scavenging was found to be 51.4% for *Coccinia grandis* pulp, while DPPH radical scavenging was found to be 21.61% at the same concentration. This finding is similar to our study in that the

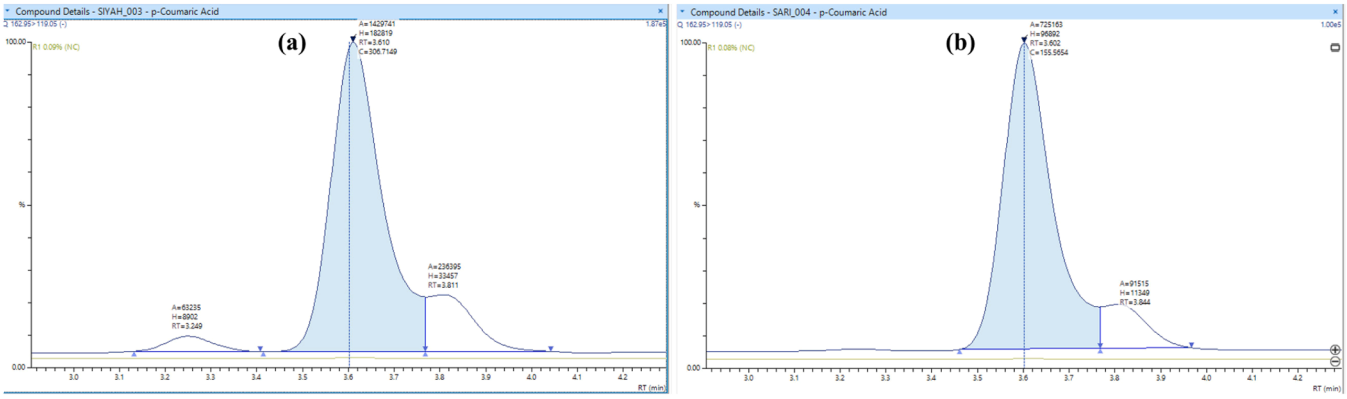

Fig. 1. LC-MS/MS chromatograms of *p*-coumaric acid detected in *Byrona aspera* extracts: (a) aerial part extract (retention time: 3.61 min); (b) root extract (retention time: 3.60 min).

Table 2
Antioxidant as radical scavenging (DPPH and ABTS) and α-glucosidase inhibitory activities of *B. aspera* extracts.

Inhibitors	[a]DPPH IC_{50} (mg/mL)	R^2	[a]ABTS IC_{50} (mg/mL)	R^2	α-Glu IC_{50} (mg/mL)	R^2
Root Extract	3.877 ± 0.059	0.954	0.457 ± 0.027	0.948	0.044 ± 0.003	0.990
Aerial Part Extract	0.678 ± 0.005	0.997	0.173 ± 0.009	0.969	0.022 ± 0.002	0.998
p-Coumaric Acid	0.563± 0.004	0.985	0.0003 ± 0.000	0.997	0.439 ± 0.026	0.999
[b]Acarbose	-	-	-	-	0.166 ± 0.007	0.992
[c]Trolox	0.006 ± 0.000	0.991	0.003 ± 0.000	0.997	-	-

[a] Values are expressed as radical scavenging activity with IC_{50}.
[b] Reference compounds used for positive control as enzyme inhibitors.
[c] Reference antioxidant (trolox) used for positive control. Values are expressed as mean ± standard deviation (SD) of three independent experiments ($n = 3$) for radical scavenging activity and α-glucosidase inhibitory activities with IC_{50}. Statistical significance was evaluated by one-way ANOVA followed by Student's *t*-test, and differences were considered significant at $p < 0.05$. The R^2 values were calculated using GraphPad Prism based on non-linear regression analysis of dose–response curves. These values indicate the goodness of fit and confirm the reliability of the calculated IC_{50} values.

extracts are more effective in scavenging ABTS radicals [39]. In a study conducted to determine the DPPH radical scavenging capacity of the methanolic extract of *Coccinia grandis* leaves, the IC_{50} value was found to be 0.50 mg/mL [40]. It is observed that a relatively similar result was obtained with the IC_{50} value (0.678 mg/mL) in the DPPH analysis of the aerial part extract in our study. In another study measuring the ABTS radical scavenging capacity of the methanol extract of *Charmaghaz sativus* seed, the IC_{50} value was determined to be 0.161 mg/mL [41]. Similar results (IC_{50}=173 mg/mL) were obtained in our ABTS radical scavenging test with aerial part extract. Consequently, it can be said that the findings are consistent with the literature.

The inhibitory effects of the extracts against α-glucosidase, a key enzyme in carbohydrate digestion, were also evaluated. The IC_{50} values for the root extract, aerial extract, p-coumaric acid, and the positive control acarbose against α-glucosidase were 0.044, 0.022, 0.439 and 0.166 mg/mL respectively (Table 2).These results indicate that both extracts exhibited stronger α-glucosidase inhibitory activity than acarbose, with the aerial extract being approximately twice as potent as the root extract. In the literature, in a study investigating the potential inhibitory effect of hydroethanol extract of *Withania frutescens* leaves on α-glucosidase activities using *in vitro* methods, an IC_{50} value of 0.18 mg/mL was reported [42]. In our study, both the root part extract (IC_{50}=0.044 mg/mL) and the aerial part extract (IC_{50}=0.022 mg/mL) showed higher inhibition against α-glucosidase. In a study investigating the α-glucosidase inhibition capacity of *Tamarix nilotica* aqueous extract, it was found that the aerial part extract in our study had a similar inhibitory effect with an IC_{50} value of 0.025 mg/mL [43].

This highlights the high therapeutic potential of *B. aspera*, particularly its aerial part, as a natural source of antidiabetic agents. The observed biological activities can be partially explained by the phytochemical composition determined via LC-MS/MS. Both extracts were rich in p-coumaric acid a compound known to contribute significantly to antioxidant and α-glucosidase inhibitory properties. Additional phenolics detected included gallic acid (20.43 mg/kg), caffeic acid (16.01 mg/kg), chlorogenic acid (11.36 mg/kg), rutin (8.08 mg/kg), naringenin (0.92 mg/kg), and galangin (0.37 mg/kg). Many of these compounds, especially p-coumaric acid, are recognized as radical scavengers and α-glucosidase inhibitors, suggesting a synergistic effect that enhances the overall activity of the extracts.

These findings indicate that *B. aspera* is a promising natural source, particularly for its aerial part extracts, in terms of *in vitro* α-glucosidase inhibition and antioxidant capacity. The observed biological activities can be partially explained by the phytochemical composition determined by LC-MS/MS. Although both extracts are rich in p-coumaric acid, the α-glucosidase inhibition potential of pure p-coumaric acid (IC_{50} = 0.439 mg/mL) was found to be approximately 20 times weaker than that of the entire aerial part extract (IC_{50} = 0.022 mg/mL). This significant difference suggests that the observed inhibitory activity of the extract is largely dependent not on a single compound but on synergistic interactions among the phenolic components. The other identified phenolics—gallic acid (20.43 mg/kg), caffeic acid (16.01 mg/kg), chlorogenic acid (11.36 mg/kg), rutin (8.08 mg/kg), naringin (0.92 mg/kg), and galangin (0.37 mg/kg) can be considered potential components contributing to this synergistic effect.

In conclusion, the aerial extract exhibited stronger antioxidant and α-glucosidase inhibitory activities than the root extract, which can be attributed to its richer and more diverse phenolic composition. Both extracts were more potent α-glucosidase inhibitors than acarbose, emphasizing their potential as natural sources of enzyme inhibitors. These findings, together with the notable activity of p-coumaric acid and the presence of other phenolic constituents, support the view that phenolic compounds collectively play a major role in the bioactivity of *B. aspera*.

2.3. Molecular docking studies

To elucidate the contribution of these identified compounds to the α-glucosidase inhibitory activity, molecular docking studies were conducted. Each compound was docked into the active site of the α-glucosidase enzyme to evaluate their binding affinity and interaction profiles.

By analyzing ligand–protein interactions (LPI) and binding energies, the compound exhibiting the strongest binding capacity was proposed as the potential active inhibitor responsible for the observed *in vitro* activity. Induced Fit Docking (IFD) was used to account for the flexibility of both the ligand and the α-glucosidase binding site, enabling accurate prediction of binding modes [44,45]. To further refine these results, MM-GBSA calculations were performed to estimate the binding free energies of the ligand–protein complexes, providing insight into their stability and interaction strength. The molecular docking and MM-GBSA ΔG binding results were summarized in Table 3.

Among the phytochemicals detected in the extracts, p-coumaric acid exhibited the most favorable interaction with α-glucosidase, with the lowest docking score (−7.783 kcal/mol) and MM-GBSA binding energy (−47.76 kcal/mol). Notably, this compound was also the most abundant in the extracts (306.71 mg/kg), strongly suggesting it is the major contributor to the observed α-glucosidase inhibitory activity. Caffeic acid and chlorogenic acid also showed relatively strong binding affinities (ΔG: −40.45 and −41.12 kcal/mol, respectively), and were present in moderate amounts.

These compounds may contribute synergistically to the α-glucosidase inhibitory effect, albeit to a lesser extent compared to p-coumaric acid. Other compounds, such as gallic acid, naringenin, galangin, and rutin, showed weaker binding energies and were present in lower concentrations, indicating a more limited role in the overall inhibitory activity.

Caffeic acid and p-coumaric acid share a similar structural backbone, with caffeic acid differing only by the presence of an additional hydroxyl group on the aromatic ring. Despite this minor difference, both compounds exhibited comparable docking behavior, suggesting that this structural motif may play a significant role in binding to the α-glucosidase active site.

The 2D and 3D ligand-protein interactions (LPI) between p-coumaric acid and α-glucosidase are illustrated in Fig. 2. Fig. 2a illustrates key hydrogen bonding and electrostatic interactions contributing to the stability of the p-coumaric acid–α-glucosidase complex. The phenolic hydroxyl group of p-coumaric acid forms two hydrogen bonds with Gly-228 and Tyr-389, while the carboxylate group forms a salt bridge and two additional hydrogen bonds with Arg-200. Furthermore, Arg-400 establishes an additional hydrogen bond with the carboxylate anion. These interactions collectively enhance the binding affinity and contribute to the stabilization of the LPI complex, thereby potentially strengthening the inhibitory effect.

Fig. 2b depicts these interactions in 3D. Yellow dashed lines represent hydrogen bonds, and the pink dashed line indicates the salt bridge interaction. The hydrogen bond lengths range from 1.76 Å to 2.72 Å. The bluish molecular surface represents the ligand binding surface, while the gray surface corresponds to the protein's binding site. The high degree of surface complementarity suggests a well-fitted ligand orientation within the active site. The three-point hydrogen bonding network further supports the structural stability of the complex.

As a conclusion, molecular docking studies demonstrated that p-coumaric acid is the most potent α-glucosidase inhibitor among the major phytochemicals identified in the extracts. Its strong binding affinity, supported by multiple hydrogen bonds and a salt bridge, along with its high abundance, suggests that it plays a central role in the observed *in vitro* α-glucosidase inhibitory activity. The close structural similarity between p-coumaric acid and caffeic acid also indicates that the phenylpropanoid scaffold is critical for effective enzyme binding.

Table 3
Molecular docking and MM-GBSA ΔG binding free energies of major compounds detected in the extracts.

Compounds	*α-Glucosidase (PDB ID: 3WY1)*	
	Docking Scores (kcal/mol)	MM-GBSA ΔG bind. (kcal/mol)
Caffeic acid	−7.351	−40.45
Chlorogenic acid	−6.226	−41.12
Galangin	−5.487	−39.03
Gallic acid	−6.477	−36.07
Naringenin	−6.038	−32.21
***p*-Coumaric acid**	**−7.783**	**−47.76**
Rutin	−5.308	−35.42

2.4. MM-GBSA Energy decomposition analysis

To gain a deeper understanding of the binding affinity and the energetic contributions of individual phytochemicals identified in *B. aspera* extracts, MM-GBSA (Molecular Mechanics Generalized Born Surface Area) energy decomposition analysis was performed. This approach allows for the breakdown of the total binding free energy (ΔG Bind) into its major energetic components, including Coulombic, covalent, hydrogen bonding, lipophilic, solvation, and van der Waals (vdW) interactions. Such decomposition provides valuable insights into the molecular determinants of ligand–protein interactions, highlighting which forces predominantly drive or destabilize the binding process [46].

The refined MM-GBSA decomposition analysis (Table 4) highlighted significant differences in the binding behaviors of the studied phytochemicals. Van der Waals and lipophilic interactions were identified as the main stabilizing factors across most ligands, particularly for p-coumaric acid and chlorogenic acid, which combined strong vdW and hydrophobic contributions. Caffeic and gallic acids benefited additionally from hydrogen bonding (–4.01 and –6.44 kcal/mol, respectively), reflecting their hydroxyl-rich structures. Galangin, despite an unfavorable solvation energy (+33.12 kcal/mol), maintained stability through compensatory vdW and hydrophobic effects. Electrostatic interactions were generally unfavorable, especially in chlorogenic (+103.32 kcal/mol) and gallic acid (+83.01 kcal/mol), but these penalties were largely offset by favorable solvation terms. Overall, p-coumaric, chlorogenic, and caffeic acids emerged as the most promising ligands, stabilized predominantly by vdW and hydrophobic forces, while gallic acid's notable hydrogen bonding also contributed to its activity. These findings provide mechanistic insight into the strong binding and potential α-glucosidase inhibitory effects of *B. aspera* phytochemicals. Overall, the results indicate that p-coumaric acid is the most potent and abundant α-glucosidase inhibitor in the extract, making it a strong candidate for further pharmacological investigation.

2.5. Molecular dynamics simulations

A 250 ns MD simulation of the p-coumaric acid–α-glucosidase complex showed stable RMSD and RMSF trajectories for both protein and ligand, indicating structural equilibrium throughout the simulation (Fig. 3). Interaction histogram analysis confirmed that key hydrogen bonds and hydrophobic contacts were largely maintained. These findings demonstrate that p-coumaric acid forms a stable and energetically favorable complex, reinforcing its potential as an α-glucosidase inhibitor.

Fig. 3a illustrates the key ligand–protein interactions observed throughout the MD simulation in a 2D representation, with the duration of each interaction expressed as a percentage of the simulation time. The carboxylic acid group of p-coumaric acid formed multiple hydrogen bonds, indicating a stable binding throughout the simulation. Notably, interactions were observed with Asp-202 (43% of the simulation), His-332 (91%), Arg-200 (177%), Arg-400 (99%), and Asp-62 (99%). The percentage exceeding 100% for Arg-200 reflects the simultaneous engagement of multiple functional groups within the residue. Additionally, the phenolic hydroxyl group formed a hydrogen bond with Gly-228 for 95% of the simulation, further stabilizing the complex.

Fig. 3b shows the RMSD profiles for both the protein and ligand atoms. The protein Cα atoms exhibited an average RMSD of 1.05 Å (light blue), ligand atoms averaged 1.5 Å (red), and the ligand relative to its initial position showed an RMSD of 0.6 Å (pink), indicating minimal

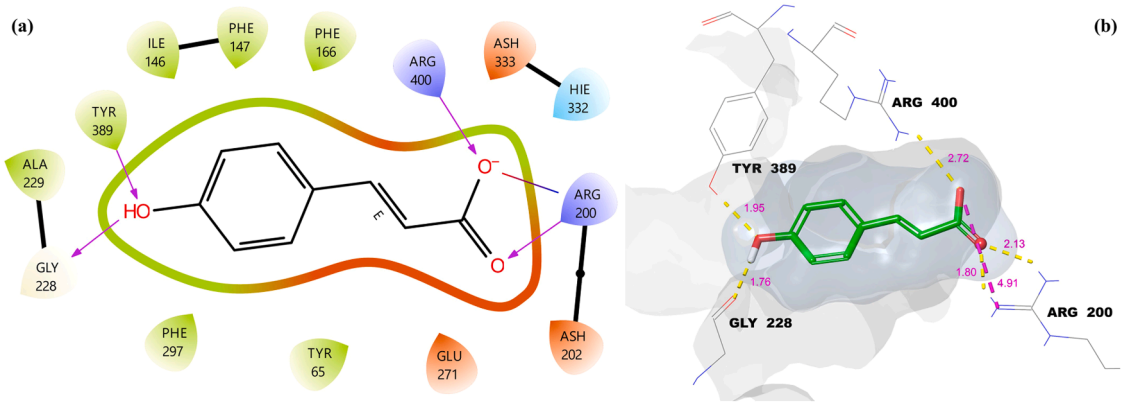

Fig. 2. The molecular docking 2D (a) and 3D (b) LPI between p-coumaric acid and α-glucosidase.

Table 4
MM-GBSA Energy decomposition analysis of phytochemicals from *Bryonia aspera* extracts.

MM-GBSA Par. (kcal/mol)	Caffeic acid	Chlorogenic acid	Galangin	Gallic acid	Naringenin	p-Coumaric acid
MMGBSA ΔG Bind Coulomb	81.97	103.32	−20.71	83.01	−4.96	90.63
MMGBSA ΔG Bind Covalent	0.74	10.74	5.39	7.18	9.16	2.01
MMGBSA ΔG Bind Hbond	−4.01	−2.70	−0.89	−6.44	−1.56	−3.85
MMGBSA ΔG Bind Lipo	−12.53	−20.13	−11.12	−7.17	−8.78	−10.75
MMGBSA ΔG Bind Solv GB	−62.78	−59.50	33.12	−74.35	22.65	−58.04
MMGBSA ΔG Bind vdW	−22.87	−42.71	−23.58	−16.78	−27.71	−27.00

conformational drift. Figs. 3c and 3d depict RMSF values for protein Cα and ligand atoms, respectively. The average RMSF for the protein was 0.8 Å, while the ligand RMSF averaged 0.7 Å, suggesting overall structural stability. In Fig. 3c, vertical green lines indicate residues in contact with the ligand, totaling 14 contacts. Finally, Fig. 3e presents the fraction interaction histogram, with green representing hydrogen bonds and purple indicating hydrophobic contacts. The most frequent interactions involved Arg-200, followed by Asp-62, Gly-228, His-332, Arg-400, and Phe-166, underscoring the critical residues that maintain strong and persistent ligand–protein binding. As a result, these analyses confirm that p-coumaric acid establishes a stable and robust complex with α-glucosidase, driven by strong and multiple hydrogen bonding interactions.

2.6. ADME Prediction

To assess the pharmacokinetic potential of major *B. aspera* phytochemicals, *in silico* ADME predictions were performed. Key parameters included Lipinski's Rule of Five, Rule of Three, human oral absorption (%HOA), Caco-2 and MDCK permeability, blood–brain barrier penetration (QPlogBB), lipophilicity (QPlogPo/w), solubility (QPlogS), hydrogen bond counts, and molecular weight, providing insight into drug-likeness, bioavailability, and permeability.

As summarized in Table 5, most compounds complied well with Lipinski's rule of five, except chlorogenic acid (1 violation) and rutin (3 violations), indicating generally favorable oral bioavailability. Rule of Three violations were minimal, suggesting potential lead-likeness. Human oral absorption (%HOA) was highest for galangin (77%) and p-coumaric acid (67%), while chlorogenic acid (17%) and rutin (0%) showed poor predicted absorption. Caco-2 and MDCK permeability values indicated moderate to good intestinal permeability for naringenin, galangin, and p-coumaric acid, whereas chlorogenic acid and rutin were low. Predicted BBB penetration (QPlogBB) was limited for all compounds, and QPlogPo/w values suggested balanced lipophilicity favoring membrane permeation for galangin and naringenin. Solubility (QPlogS) was moderate, higher for caffeic acid and p-coumaric acid compared to lipophilic galangin. Hydrogen bond counts were generally within acceptable ranges, except for rutin, correlating with its poor permeability and solubility. Molecular weights were suitable for oral drugs, except rutin (610.52 g/mol). Overall, p-coumaric acid, galangin, and naringenin exhibited favorable ADME profiles, supporting their potential as orally active α-glucosidase inhibitors, whereas chlorogenic acid and rutin may be limited by poor absorption and low permeability.

2.7. Molecular docking validations

Docking validation was performed by redocking the co-crystallized ligand into the α-glucosidase active site (PDB ID: 3WY1; resolution: 2.00 Å). The superposition of the co-crystallized ligand (green) and redocked pose (pink) showed good agreement, with an RMSD of 1.31 Å (Fig. 4). As the RMSD value was below 2.0 Å, the docking protocol was considered reliable [44,45].

3. Conclusion

This study comprehensively evaluated the phenolic composition, antioxidant potential, and α-glucosidase inhibitory properties of *B. aspera* extracts through integrated *in vitro* and *in silico* approaches. LC-MS/MS analysis revealed seven major phenolic constituents, caffeic acid, chlorogenic acid, galangin, gallic acid, naringenin, p-coumaric acid, and rutin, with p-coumaric acid being the most abundant in both aerial (306.71 mg/kg) and root (155.56 mg/kg) extracts.

In biological assays, both extracts showed strong antioxidant and α-glucosidase inhibitory activities, with the aerial extract being the most potent (IC_{50} = 0.678, 0.173, and 0.022 mg/mL for DPPH, ABTS, and α-glucosidase, respectively). The root extract showed moderate activity, while ***p*-coumaric acid** displayed high antioxidant potential (IC_{50} = 0.563 and 0.0003 mg/mL) but weaker α-glucosidase inhibition (IC_{50} = 0.439 mg/mL). Its high abundance and strong antioxidant capacity likely enhance the overall bioactivity of *B. aspera* through synergistic effects with other phenolics.

Molecular docking and MM-GBSA analyses confirmed this relationship at the molecular level. p-Coumaric acid exhibited the lowest docking score (–7.783 kcal/mol) and the most favorable binding free

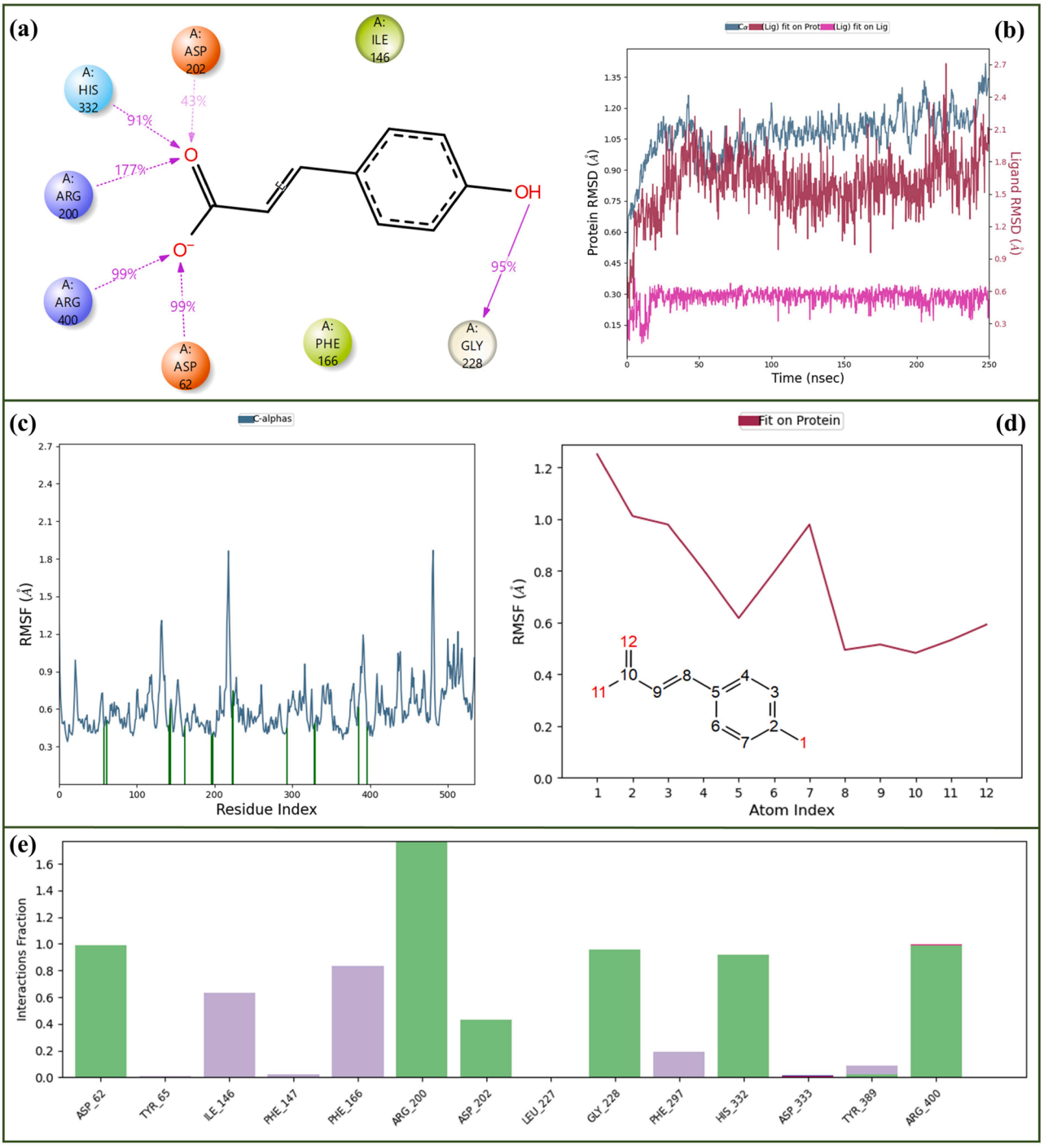

Fig. 3. The 250 ns MD analysis of the p-coumaric acid–α-glucosidase complex: (a) key ligand–protein interactions with simulation duration (%), (b) RMSD of protein Cα (light blue), ligand (red), and ligand relative to initial position (pink), (c,d) RMSF of protein Cα and ligand atoms (e) fraction interaction histogram showing hydrogen bonds (green) and hydrophobic contacts (purple). (For interpretation of the references to color in this figure legend, the reader is referred to the web version of this article.).

energy (ΔG = –47.76 kcal/mol) against α-glucosidase, outperforming other major compounds such as caffeic acid (–7.351, –40.45 kcal/mol) and chlorogenic acid (–6.226, –41.12 kcal/mol). The strong binding affinity of p-coumaric acid was stabilized by multiple hydrogen bonds and hydrophobic contacts with critical catalytic residues, particularly Asp-62, Arg-200, Gly-228, His-332, and Arg-400. A 250 ns molecular dynamics simulation verified the stability of the p-coumaric acid–α-glucosidase complex, with average RMSD values of 1.05 Å for protein Cα and 1.5 Å for ligand atoms, and persistent hydrogen bonding (>90% occupancy) throughout the trajectory. MM-GBSA energy decomposition further revealed that van der Waals (–36.81 kcal/mol) and lipophilic (–20.95 kcal/mol) terms were the primary stabilizing factors, confirming the strong nonpolar interactions responsible for the ligand's high affinity. In silico ADME prediction supported these findings, indicating good oral absorption (67%), balanced lipophilicity (QPlogPo/w = 2.9), and full compliance with Lipinski's rule of five, suggesting favorable pharmacokinetic properties for p-coumaric acid.

Collectively, the integrated data suggest that p-coumaric acid is one

Table 5
ADME Prediction of the title compounds.

Parameters	Naringenin	Gallic acid	Chlorogenic acid	Caffeic acid	p-Coumaric acid	Galangin	Rutin	Ref. Values
Rule of Five	0	0	1	0	0	0	3	Max 4 violation
Rule of Three	0	1	1	1	0	0	2	Max 3 violation
%HOA	74	41	17	54	67	77	0	>80 high, <25 poor
QPPCaco	128	9	1	22	61	168	1	<25 poor, >500 great
QPPMDCK	54	4	1	10	31	72	1	<25 poor, >500 great
QPlogBB	−1.416	−1.679	−3.342	−1.547	−1.082	−1.308	−3.865	–3 to 1.2
QPlogPo/w	1.627	−0.574	−0.232	0.541	1.429	1.777	−2.500	–2 to 6.5
QPlogS	−3.438	−0.712	−2.589	−1.288	−1.665	−3.411	−1.656	–6.5 to 0.5
Accept HB	4	4	10	4	3	4	20	2 to 20
Donor HB	2	4	6	3	2	2	9	0 to 6
mol MW	272.25	170.12	354.31	180.16	164.16	270.24	610.52	130 to 725

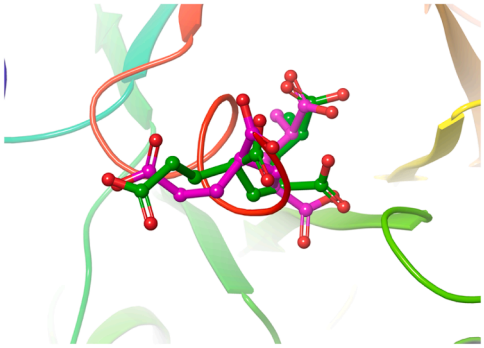

Fig. 4. Docking validation: superposition of co-crystallized (green) and redocked (pink) ligands. (For interpretation of the references to color in this figure legend, the reader is referred to the web version of this article.).

of the major contributors to the observed antioxidant and α-glucosidase inhibitory effects of *B. aspera*, likely acting in combination with other phenolic constituents through synergistic effects. Its high abundance, strong binding affinity, stable complex formation, and favorable ADME profile highlight its potential as a promising lead natural compound for α-glucosidase inhibition. Although the findings of this study are promising, validation through cell-based and *in vivo* experimental models is required to substantiate any clinical antidiabetic claims. Therefore, future studies may focus on evaluating the antihyperglycemic activity of *B. aspera* and p-coumaric acid in streptozotocin-induced diabetic animal models and elucidating the precise inhibition kinetics and mechanism of enzyme inhibition.

4. Materials and method

4.1. Chemicals and plant materials

In LC–MS/MS analysis, the following compounds were used as standards: gallic acid (97.5%), quercetin (95%), catechin hydrate (99%), oleuropein (98%), p-coumaric acid (98%), chlorogenic acid (96%), pinocembrin (95%), hesperetin (95%), caffeic acid (98%), myricetin (96%), kaempferol (97%), apigenin (95%), naringenin (98%), CAPE (97%), chrysin (98%), galangin (95%), genistein (98%), rutin hydrate (≥94%), formic acid, which were purchased from Sigma Aldrich. Ethanol and HPLC-grade methanol were purchased from Merck (Germany). Stock solutions (1000 mg/L) were prepared from each phenolic standard in MeOH. Working solutions were prepared at 1 mg/L by taking appropriate portions from the stock solutions. The compounds used for antioxidant activity such as 1,1-diphenyl-2-picryl-hydrazyl (DPPH), 2,2′-azino-bis(3-et hylbenzthiazoline-6-sulfonic acid) (ABTS), and α-tocopherol were obtained from Sigma (Sigma–Aldrich, Germany). Dilutions were carried out employing automated pipettes and precision glass volumetric flasks. All remaining chemicals utilized were of analytical grade and sourced from Sigma–Aldrich or Merck. The plant was collected during the flowering period (*Bryonia aspera*, B7 Tunceli Center (Türkiye), Mazgirt district, Güneşdere neighborhood, at the streambank, May 2024, Voucher specimen: MA 2046), dried under appropriate conditions and turned into a herbarium specimen at Munzur University laboratories.

4.2. Preparation of Bryonia aspera extracts

Ethanol extraction of *B. aspera* was carried out in Soxhlet extractor setup. For this purpose, the aboveground (AG: stem and flower) and underground (UG: root) parts of Bryonia Aspera were dried separately in the NUVE heating oven (FN 055 Series) at 30 °C. Plant materials were ground into a fine powder in a blender. The solid to be extracted (ground plant material; AG/UG; 25 g/25 g) is placed on cartridge paper (made from cellulose). 250 mL of ethanol was added to the reactor, and the system was heated. Extraction was performed by siphoning the solvent three times through the Sohxlet apparatus. The ethanol solvent was removed via a rotary evaporator (Heidolph Hei-Vap Adv ML) at 40 °C to obtain a dry extract. The dried ethanolic extract was stored in a glass bottle at −20 °C until further use [4,47,48].

4.3. Instruments and chromatographic conditions

4.3.1. LC-MS/MS Analysis

LC–MS/MS analyses of the samples were performed as in our previous studiesc (Oren, et all., 2024). Binary gradient LC-40D XS- Autosampler Model; SIL-40C XS- Oven Model; the system was coupled to an CTO-40S-Shımadzu 8050 triple quadruple detector (Shimadzu, Japan) controlled by LabSolution 5.60 SP2 software. A Shimadzu Nexera X2 UHPLC (Shimadzu, Japan) liquid chromatograph equipped with an Inert Sustain Swift C18 (2.1 mm*100 mm, 3 μm) column was used. Ultra-pure water was prepared on a Milli-Q IQ 7000 system (Millipore Company, USA). A liquid chromatograph-mass spectrometer (LC–MS/MS) was used to analyze 18 distinct phenolic compounds [49–51].

4.3.2. Sample preparation

0.01 g sample (accuracy of 0.001 g) is weighed into a 50 ml centrifuge tube. 15 ml methanol and 15 ml water are added. The sample is then subjected to ultrasonication for 20 min. It is then centrifuged at 4000 rpm for 10 min. After centrifugation, the sample is made up to 50 ml methanol. It is then passed through a filter paper and a 0.45 μm filter tip before being transferred to a vial for LC-MS/MS analysis.

4.3.3. MS Parameters

Table 6.

4.3.4. Validation parameters

During the experiments, the samples were kept at 15 °C in the autosampler. Additionally, the chromatographic conditions, instrumental procedure optimization, linearity, repeatability, recovery, precision, limits of quantification (LOQ) and determination (LOD),

Table 6
MS parameters for the tested compounds.

Standart Compounds	Precursor	Product	CE	Polarity
Gallic acid	168.9	125	15	Negative
Catechin Hydrate	290.8	139	−13	Positive
	290.8	123	−21	Positive
Chlorogenic acid	353.3	191.3	17	Negative
	353.3	111	32	Negative
Cafeic acid	178.85	135.05	16	Negative
	178.85	89.2	33	Negative
p-Coumaric Acid	162.95	93	28	Negative
	162.95	119.5	15	Negative
Hesperidin	609	301.2	25	Negative
Rutin	608.9	300	36	Negative
	608.9	271.05	55	Negative
Oleuropein	539.3	275.1	21	Negative
	539.3	306.9	21	Negative
Myricetin	317	151.2	24	Negative
	317	179.2	12	Negative
Naringenin	272.8	153	−24	Positive
	272.8	147.1	−21	Positive
Quercetin	300.8	179	18	Negative
	300.8	151	21	Negative
Kemferol	285.2	116.9	45	Negative
	285.2	93	36	Negative
	285.2	182	49	Negative
	285.2	227.2	33	Negative
Apigenin	269.1	117	33	Negative
	269.1	149.2	22	Negative
Genistein	269.1	117.1	48	Negative
	269.1	106.9	30	Negative
Pinosembrin	254.9	213.1	19	Negative
	254.9	151.2	21	Negative
CAPE	282.85	135.05	25	Negative
	282.85	161	23	Negative
	282.85	179.05	18	Negative
Chrysin	252.8	209.15	22	Negative
	252.8	143.1	26	Negative
	252.8	62.95	31	Negative
Galangin	269.2	213.1	24	Negative
	269.2	227	25	Negative

identification of uncertainty sources, and identification of standard uncertainties (Table 7) were performed according to our previous study [52].

4.4. Antioxidant and α-glucosidase inhibitory activity studies

4.4.1. DPPH Radical scavenging activity

The DPPH assay was used to determine the free radical scavenging activity of the extracts. 0.9 mL of DPPH (0.1 mM) solution was mixed with 0.1 mL of extract at different concentrations or positive control trolox. The reaction mixture was incubated in the dark for 30 min, and absorbance was measured at 517 nm. 1 mL of methanol was used as a blank. The negative control mixture contained 0.9 mL of DPPH and 0.1 mL of methanol. The initial sample/standard stock solutions were prepared in methanol at a concentration of 5 mg/mL, and serial dilutions were prepared to cover a concentration range spanning at least two orders of magnitude around the expected IC_{50} values. The decrease in absorbance was considered as stronger DPPH radical scavenging activity [12,53,54].

4.4.2. ABTS Radical scavenging activity

ABTS+ radical scavenging activity of the extracts was conducted according to previously described literature [12]. Briefly, equal volumes of ABTS+ solution (7.0 mM) and potassium persulfate (2.45 mM) were mixed and left in the dark for 16 h to allow the formation of the ABTS+ radical cation. Furthermore, the ABTS+ solution was adjusted by diluting with methanol until its absorbance reached 0.70 ± 0.10 at 734 nm. Then, 0.1 mL of samples prepared at different concentrations or trolox (as a reference standard) was mixed with 0.9 mL of the diluted ABTS+ solution. Finally, the test mixtures were left at room temperature for 6 min, and the absorbance was measured at 734 nm. 1 mL of methanol was used as a blank. The negative control mixture contained 0.9 mL of ABTS and 0.1 mL of ethanol [55,56].

4.4.3. In vitro α-glucosidase inhibitory activity

The α-glucosidase inhibitory activity of the extracts as antidiabetic activity was evaluated using a modified α-glucosidase inhibition assay based on the method previously described by Yadav and coworkers [12]. Initial sample/standard stock solutions were prepared in DMSO at a concentration of 5 mg/mL, and serial dilutions were prepared to cover a concentration range spanning at least two orders of magnitude around the expected IC_{50} values. Briefly, 100 μL of extract at a range of concentrations was mixed with 50 μL of α-glucosidase solution (1 U/mL) and pre-incubated at room temperature for 5 min. The tested concentrations were selected to cover a broad range of inhibition levels, allowing accurate determination of IC_{50} values. Subsequently, 150 μL of p-nitrophenyl-α-D-glucopyranoside (pNPG, 5 mM) was added as the substrate, and the reaction mixture was further incubated for 5 min. The reaction was terminated by adding 500 μL of sodium carbonate solution (200 mM). The release of p-nitrophenol was measured at 405 nm using a UV spectrophotometer. Acarbose was used as a positive control. All experiments were performed in triplicate [57,58].

Table 7
Bryonia aspera content's uncertainty and validation parameters.

Phenolic Compounds	Linearity (R^2)	LOD (μg/kg)	LOQ (μg/kg)	Intra-Day Variation (%RSD) (100–200 750 μg/kg	Inter-Day Variation (%RSD) (100–200–750 μg/kg	Recovery (%) (100–200–750 μg/kg
Gallic acid	0.998	0.03	0.1	8–9–7	10–9–8	87–90–95
Catechin hydrate	0.999	0.03	0.11	10–8–9	11–10–9	82–88–92
Chlorogenic acid	0.998	0.05	0.12	9–10–8	10–10–9	85–89–93
Caffeic acid	0.999	0.04	0.09	8–9–8	9–8–8	90–92–96
p-Coumaric acid	0.998	0.05	0.08	10–9–8	11–10–9	88–91–94
Hesperidin	0.999	0.04	0.1	8–8–7	8–7–8	92–95–98
Rutin	0.999	0.04	0.12	9–10–9	10–9–10	86–89–92
Oleropin	0.998	0.03	0.09	8–9–8	9–8–9	88–90–93
Myricetin	0.999	0.05	0.11	10–9–9	10–9–8	85–90–94
Naringenin	0.999	0.06	0.1	9–8–8	10–9–9	83–87–91
Quercetin	0.998	0.05	0.12	9–9–8	10–9–9	87–92–95
Kaempferol	0.999	0.03	0.08	8–9–9	9–8–8	89–91–94
Apigenin	0.998	0.06	0.11	9–8–9	10–8–9	86–89–93
Genistein	0.999	0.04	0.09	8–9–8	8–7–7	93–95–98
Pinocembrin	0.999	0.04	0.1	10–8–8	10–9–8	87–91–94
CAPE	0.998	0.05	0.11	8–9–8	9–8–9	95–97–99
Chrysin	0.999	0.05	0.09	9–8–8	10–9–8	86–90–92
Galangin	0.998	0.03	0.08	10–9–7	11–10–8	89–91–95

4.5. Computational studies

Molecular docking and molecular dynamics (MD) simulations were performed using the Schrödinger Molecular Modeling Suite (2025–1) with the Maestro interface (v14.5) and Desmond. The crystal structure of α-glucosidase (PDB ID: 3WY1) was retrieved from the Protein Data Bank and prepared using the Protein Preparation Wizard. Missing side chains and loops were added where necessary, hydrogen atoms were assigned, bond orders were corrected, and protonation states were generated using Epik at pH 7.0 $\pm$ 2.0. The hydrogen-bonding network was optimized, and restrained energy minimization was performed using the OPLS4e force field with a heavy atom convergence threshold of 0.3 Å.

Ligands were prepared using LigPrep to generate low-energy 3D conformations. Possible ionization states at physiological pH (7.0 $\pm$ 2.0) were generated using Epik, and geometries were optimized with the OPLS4e force field. The receptor grid was generated by centering the grid box on the co-crystallized ligand binding site. The grid box dimensions were defined as 20 $\times$ 20 $\times$ 20 Å for the outer box and 10 $\times$ 10 $\times$ 10 Å for the inner box, ensuring full coverage of the active site residues. Van der Waals scaling factors were set to 1.0 with a partial charge cutoff of 0.25.

Docking simulations were carried out using Glide in extra precision (XP) mode. For each ligand, up to 20 poses were generated, and the best-ranked conformations were selected based on GlideScore and IFD score. Receptor flexibility was further considered using the Induced Fit Docking (IFD) protocol, allowing side-chain refinement within 5.0 Å of the ligand. The top-ranked complexes were subjected to Prime MM-GBSA calculations using the VSGB solvation model and OPLS4e force field to estimate binding free energies.

MD simulations were performed using Desmond. Each protein–ligand complex was placed in an orthorhombic simulation box with a buffer distance of 10 Å and solvated using the TIP4P water model. The system was neutralized with appropriate counter ions, and 0.15 M NaCl was added to mimic physiological ionic strength. Long-range electrostatic interactions were treated using the Particle Mesh Ewald (PME) method with a cutoff radius of 9.0 Å for short-range interactions. Energy minimization was followed by a two-stage equilibration protocol under NVT and NPT ensembles. The production MD simulation was carried out for 250 ns at 300 K and 1.01325 bar using the Nosé–Hoover thermostat and Martyna–Tobias–Klein barostat. The integration time step was set to 2.0 fs, and coordinates were recorded at appropriate intervals for analysis. Trajectory analyses were conducted using the Simulation Interaction Diagram tool in Desmond. Structural stability and flexibility were evaluated through root mean square deviation (RMSD) and root mean square fluctuation (RMSF) analyses. Key intermolecular interactions, including hydrogen bonds, hydrophobic contacts, ionic interactions, and water bridges, were monitored throughout the simulation [59–62].

4.6. Statistical analysis

Statistical analysis was performed using one-way analysis of variance (ANOVA) followed by Student's *t*-test to evaluate differences between groups. All experiments were conducted in triplicate, and the results are expressed as mean $\pm$ standard deviation (SD). A value of $p < 0.05$ was considered statistically significant [63,64].

CRediT authorship contribution statement

Salih Tuncay: Writing – review & editing, Writing – original draft, Visualization, Investigation, Formal analysis, Conceptualization. **Ömer Faruk Karasakal:** Investigation, Formal analysis, Data curation. **Mikail Açar:** Investigation, Formal analysis, Data curation. **İsra Toptancı:** Investigation, Formal analysis. **Halil Şenol:** Writing – review & editing, Writing – original draft, Software, Investigation, Formal analysis, Conceptualization. **Olgun Çırak:** Investigation, Formal analysis. **Mesut Işık:** Investigation, Formal analysis. **Şükrü Beydemir:** Supervision.

Declaration of competing interest

The authors declare that they have no known competing financial interests or personal relationships that could have appeared to influence the work reported in this paper.

Acknowledgements

The authors thank Berkan Artan, Süleyman Önal, Murat Babar, and Garip Özhan for their assistance with fieldwork and ethnobotanical studies.

Data availability

No data was used for the research described in the article.

References

[1] S. Fatmawati, F. Auwaliyah, Yuliana, N. Hasanah, D.A. Putri, H. Kainama, M. I. Choudhary, Antioxidant and α-glucosidase inhibitory activities of compound isolated from Stachytarpheta jamaicensis (L) Vahl. Leaves, Sci. Rep. 13 (1) (2023) 18597, https://doi.org/10.1038/s41598-023-45357-z.
[2] C.M. Uritu, C.T. Mihai, G.-D. Stanciu, G. Dodi, T. Alexa-Stratulat, A. Luca, M.-M. Leon-Constantin, R. Stefanescu, V. Bild, S. Melnic, B.I. Tamba, Medicinal plants of the Family Lamiaceae in Pain therapy: a review, Pain Res. Manag. 2018 (1) (2018) 1–44, https://doi.org/10.1155/2018/7801543.
[3] Ö. Demirkıran, E. Erol, H. Şenol, İ.M. Kesdi, G.Ö. Alim Toraman, E.Ş. Okudan, G. Topcu, Cytotoxic meroterpenoids from brown alga Stypopodium schimperi (Kützing) Verlaque & Boudouresque with comprehensive molecular docking & dynamics and ADME studies, Process Biochem. 136 (2024) 90–108, https://doi.org/10.1016/j.procbio.2023.11.029.
[4] G.O.A. Toraman, S. Atasoy, H. Şenol, E.S. Okudan, H.O. Dinc, G. Topcu, LC-MS and GCMS– analyses on green algae penicillus capitatus: cytotoxic, antimicrobial and anticholinesterase activity screening enhanced by molecular docking & dynamics and ADME studies, Chem. Biodivers. 21 (n/a) (2024) e202400915, https://doi.org/10.1002/cbdv.202400915.
[5] S.K. Aydin, A. Ertas, M. Boga, E. Erol, G.O.A. Toraman, T.K. Saygi, B. Halfon, G. Topcu, Di-, and triterpenoids isolation and LC-MS analysis of salvia marashica extracts with bioactivity studies, Rec. Nat. Prod. 15 (6) (2021) 463–475, https://doi.org/10.25135/rnp.251.21.03.2003.
[6] A. Dey, S. Nandy, A. Mukherjee, B.K. Modak, Sustainable utilization of medicinal plants and conservation strategies practiced by the aboriginals of Purulia district, India: a case study on therapeutics used against some tropical otorhinolaryngologic and ophthalmic disorders, Environ. Dev. Sustain. 23 (4) (2021) 5576–5613, https://doi.org/10.1007/s10668-020-00833-8.
[7] I. Ismail Iid, S. Kumar, S. Shukla, V. Kumar, R. Sharma, Putative antidiabetic herbal food ingredients: nutra/functional properties, bioavailability and effect on metabolic pathways, Trends. Food Sci. Technol. 97 (2020) 317–340, https://doi.org/10.1016/j.tifs.2020.01.017.
[8] G. Paun, E. Neagu, C. Albu, S. Savin, G.L. Radu, *In* vitro evaluation of antidiabetic and anti-inflammatory activities of polyphenolic-rich extracts from Anchusa officinalis and Melilotus officinalis, ACS Omega 5 (22) (2020) 13014–13022, https://doi.org/10.1021/acsomega.0c00929.
[9] A. Singh, S. Yadav, P. Pathak, A. Verma, J.P. Yadav, Harnessing Luteolin's therapeutic potential in human disorders: medicinal significance, biological, clinical properties and analytical aspects, Pharmacol. Res. 10 (2024) 100401, https://doi.org/10.1016/j.prmcm.2024.100401.
[10] H. Wagner, G. Ulrich-Merzenich, Synergy research: approaching a new generation of phytopharmaceuticals, Phytomedicine 16 (2) (2009) 97–110, https://doi.org/10.1016/j.phymed.2008.12.018.
[11] N.R. Kokila, B. Mahesh, R. Ramu, S.G. Divakara, K. Mruthunjaya, N. Raghav, T. B. Shivanandappa, Combined *in vitro* and in silico approach to define alangimarckine from Thunbergia mysorensis leaves as a potential inhibitor of α-glucosidase, J. Biomol. Struct. Dyn. 43 (18) (2025) 10878–10897, https://doi.org/10.1080/07391102.2025.2472396.
[12] J.P. Yadav, P. Pathak, S. Yadav, A. Singh, N.N. Palei, A. Verma, In-vitro evaluation of antidiabetic, antioxidant, and anti-inflammatory activities in Mucuna pruriens seed extract, Clin. Phytosci. 10 (1) (2024) 21, https://doi.org/10.1186/s40816-024-00381-y.
[13] J.P. Yadav, A.K. Singh, M. Grishina, P. Pathak, D.K. Patel, Cucumis melo Var. Agrestis Naudin as a potent antidiabetic: investigation via experimental methods, Phytomed. Plus 2 (4) (2022) 100340, https://doi.org/10.1016/j.phyplu.2022.100340.
[14] M.M. Rosa, T. Dias, Chapter 54 - commonly used endocrine drugs, in: J. Biller, J. M. Ferro (Eds.), Handbook of Clinical Neurology, Elsevier, 2014, pp. 809–824, https://doi.org/10.1016/B978-0-7020-4087-0.00054-1.

[15] C. Türkeş, Aldose reductase with quinolone antibiotics interaction: *in vitro* and in silico approach of its relationship with diabetic complications, Arch. Biochem. Biophys. 761 (2024) 110161, https://doi.org/10.1016/j.abb.2024.110161.
[16] F.S. Tokali, Y. Demir, C. Turkes, B. Dincer, S. Beydemir, Novel acetic acid derivatives containing quinazolin-4(3H)-one ring: synthesis, *in vitro*, and in silico evaluation of potent aldose reductase inhibitors, Drug Dev. Res. 84 (2) (2023) 275–295, https://doi.org/10.1002/ddr.22031.
[17] Y. Demir, F.S. Tokalı, E. Kalay, C. Türkeş, P. Tokalı, O.N. Aslan, K. Şendil, Ş. Beydemir, Synthesis and characterization of novel acyl hydrazones derived from vanillin as potential aldose reductase inhibitors, Mol. Divers. 27 (2023) 1713–1733, https://doi.org/10.1007/s11030-022-10526-1.
[18] Y. Sivasothy, K.Y. Loo, K.H. Leong, M. Litaudon, K. Awang, A potent alpha-glucosidase inhibitor from Myristica cinnamomea King, Phytochemistry 122 (2016) 265–269, https://doi.org/10.1016/j.phytochem.2015.12.007.
[19] M. Peña, A. Guzmán, C. Mesas, J.M. Porres, R. Martínez, F. Bermúdez, C. Melguizo, L. Cabeza, J. Prados, Evaluation of the leaves and seeds of Cucurbitaceae plants as a new source of bioactive compounds for colorectal cancer prevention and treatment, Nutrients 16 (23) (2024) 4233, https://doi.org/10.3390/nu16234233.
[20] S. Chatterjee, P. Sagar, A. Singh, A. Sharma, Y.K. Mishra, D. Upadhyay, J.K. Tiwari, A. Kumar, Pre-breeding to molecular breeding for crop improvement of spine gourd (Momordica dioica Roxb.): challenges and opportunities, Euphytica 221 (10) (2025) 154, https://doi.org/10.1007/s10681-025-03599-0.
[21] B. Salehi, C. Quispe, J. Sharifi-Rad, L. Giri, R. Suyal, A.K. Jugran, P. Zucca, A. Rescigno, S. Peddio, O. Bobis, A.R. Moise, G. Leyva-Gómez, M.L. Del Prado-Audelo, H. Cortes, M. Iriti, M. Martorell, N. Cruz-Martins, M. Kumar, W. Zam, Antioxidant potential of family cucurbitaceae with special emphasis on cucurbita genus: a key to alleviate oxidative stress-mediated disorders, Phytother. Res. 35 (7) (2021) 3533–3557, https://doi.org/10.1002/ptr.7045.
[22] S. Sahranavard, F. Naghibi, S. Ghafari, Cytotoxic activity of extracts and pure compounds of bryonia aspera, Int. J. Pharm. Pharm. Sci. 4 (2012) 541–543.
[23] B. Benarba, K. Belhouala, The Genus Bryonia L. (Cucurbitaceae): a systematic review of its botany, phytochemistry, traditional uses, and biological activities, Science 6 (1) (2024) 7, https://doi.org/10.3390/sci6010007.
[24] K. Kaur, B. Ahmed, J. Singh, M. Rawat, G. Kaur, M. AlKahtani, E.A.H. Alhomaidi, J. Lee, Bryonia laciniosa linn mediated green synthesized Au NPs for catalytic and antimicrobial applications, J. King Saud Univ. Sci. 34 (4) (2022) 102022, https://doi.org/10.1016/j.jksus.2022.102022.
[25] N.R. Kokila, B. Mahesh, K.P. Roopa, B. Daruka Prasad, K. Raj, S.N. Manjula, K. Mruthunjaya, R. Ramu, Thunbergia mysorensis mediated nano silver oxide for enhanced antibacterial, antioxidant, anticancer potential and *in vitro* hemolysis evaluation, J. Mol. Struct. 1255 (2022) 132455, https://doi.org/10.1016/j.molstruc.2022.132455.
[26] B. Benarba, K. Belhouala, The Genus Bryonia L. (Cucurbitaceae): a systematic review of its botany, phytochemistry, traditional uses, and biological activities, Science 6 (2024) 7, https://doi.org/10.3390/sci6010007.
[27] I. Gouvinhas, M.J. Saavedra, M.J. Alves, J. Garcia, Exploring the impact of ultrasound-assisted extraction on the phytochemical composition and bioactivity of Tamus communis L. Fruits, Pharmaceuticals 18 (9) (2025) 1342, https://doi.org/10.3390/ph18091342.
[28] Z. Wang, Y. Jiang, C. Ge, Y. Wang, J. He, J. Chen, X. Hou, Anti-inflammatory activity evaluation and molecular docking analysis of four new compounds isolated from M. oleifera seeds, J. Mol. Struct. 1318 (2024) 139269, https://doi.org/10.1016/j.molstruc.2024.139269.
[29] S.B. Patel, D. Santani, V. Patel, M. Shah, Anti-diabetic effects of ethanol extract of Bryonia laciniosa seeds and its saponins rich fraction in neonatally streptozotocin-induced diabetic rats, Pharmacogn. Res. 7 (1) (2015) 92, https://doi.org/10.4103/0974-8490.147217.
[30] S. Patel, D. Santani, M. Shah, V. Patel, Anti-hyperglycemic and Anti-hyperlipidemic effects of Bryonia Laciniosa seed extract and its saponin fraction in streptozotocin-induced diabetes in rats, J. Young. Pharm. 4 (3) (2012) 171–176, https://doi.org/10.4103/0975-1483.100024.
[31] G. Zeng, Z. Wu, W. Cao, Y. Wang, X. Deng, Y. Zhou, Identification of anti-nociceptive constituents from the pollen of Typha angustifolia L. using effect-directed fractionation, Nat. Prod. Res. 34 (7) (2020) 1041–1045, https://doi.org/10.1080/14786419.2018.1539979.
[32] X. Chen, C. Chen, X. Fu, Hypoglycemic activity *in vitro* and vivo of a water-soluble polysaccharide from Astragalus membranaceus, Food Funct. 13 (21) (2022) 11210–11222, https://doi.org/10.1039/D2FO02298B.
[33] N.R. Kokila, B. Mahesh, R. Ramu, K. Mruthunjaya, B.K. Bettadaiah, H. Madhyastha, Inhibitory effect of gallic acid from Thunbergia mysorensis against α-glucosidase, α-amylase, aldose reductase and their interaction: inhibition kinetics and molecular simulations, J. Biomol. Struct. Dyn. 41 (20) (2023) 10642–10658, https://doi.org/10.1080/07391102.2022.2156923.
[34] F. Bagheri, S. Salami, Z. Shahsavari, M. Hatami, S. Sahranavard, Bryonia aspera root extracts induce programmed cell death in selected cell lines of glioblastoma, ovarian, and breast cancer, J. Food Biochem. 2024 (1) (2024) 1–10, https://doi.org/10.1155/2024/2217335.
[35] Y. Yesil, I. Inal, Ethnomedicinal plants of Hasankeyf (Batman-Turkey), Front. Pharmacol. 11 (2021) 624710, https://doi.org/10.3389/fphar.2020.624710.
[36] J. Peng, C. Ge, K. Shang, S. Liu, Y. Jiang, Comprehensive profiling of the chemical constituents in Dayuanyin decoction using UPLC-QTOF-MS combined with molecular networking, Pharm. Biol. 62 (1) (2024) 480–498, https://doi.org/10.1080/13880209.2024.2354341.
[37] S. Shi, K. Li, J. Peng, J. Li, L. Luo, M. Liu, Y. Chen, Z. Xiang, P. Xiong, L. Liu, W. Cai, Chemical characterization of extracts of leaves of Kadsua coccinea (Lem.) A.C. Sm. by UHPLC-Q-Exactive orbitrap mass spectrometry and assessment of their antioxidant and anti-inflammatory activities, Biomed. PharmacOther 149 (2022) 112828, https://doi.org/10.1016/j.biopha.2022.112828.
[38] M. Zhang, Y. Wang, Q. Li, Y. Luo, L. Tao, D. Lai, Y. Zhang, L. Chu, Q. Shen, D. Liu, Y. Wu, Ultrasound-assisted extraction of polysaccharides from Ginkgo biloba: process optimization, composition and anti-inflammatory activity, Heliyon 10 (18) (2024) e37811, https://doi.org/10.1016/j.heliyon.2024.e37811.
[39] K. Akhter, A. Bibi, A. Rasheed, S.u. Rehman, U. Shafique, T. Habib, Indigenous vegetables of family cucurbitaceae of Azad Kashmir: a key emphasis on their pharmacological potential, PLoS ONE 17 (6) (2022) e0269444, https://doi.org/10.1371/journal.pone.0269444.
[40] B. Salehi, C. Quispe, J. Sharifi-Rad, L. Giri, R. Suyal, A.K. Jugran, P. Zucca, A. Rescigno, S. Peddio, O. Bobiş, A.R. Moise, G. Leyva-Gómez, M.L. Del Prado-Audelo, H. Cortes, M. Iriti, M. Martorell, N. Cruz-Martins, M. Kumar, W. Zam, Antioxidant potential of family cucurbitaceae with special emphasis on cucurbita genus: a key to alleviate oxidative stress-mediated disorders, Phytother. Res. 35 (7) (2021) 3533–3557, https://doi.org/10.1002/ptr.7045.
[41] W.N. Showkat, N. Khan, N. Jamila, U. Nishan, A. Badshah, Z. Iqbal, J.Y. Jeong, K. S. Kim, Effect of gamma irradiation on the antimicrobial and free radical scavenging activities of solvents-based extracts of Cucurbitaceae seeds, Anal. Lett. 58 (9) (2025) 1436–1449, https://doi.org/10.1080/00032719.2024.2372841.
[42] H. Mechchate, I. Es-safi, A. Louba, A.S. Alqahtani, F.A. Nasr, O.M. Noman, M. Farooq, M.S. Alharbi, A. Alqahtani, A. Bari, H. Bekkari, D. Bousta, *In Vitro* alpha-amylase and alpha-glucosidase inhibitory activity and In vivo antidiabetic activity of Withania frutescens L. Foliar extract, Molecules 26 (2) (2021) 293, https://doi.org/10.3390/molecules26020293.
[43] M. Daou, N.A. Elnaker, M.A. Ochsenkühn, S.A. Amin, A.F. Yousef, L.F. Yousef, *In vitro* α-glucosidase inhibitory activity of Tamarix nilotica shoot extracts and fractions, PLoS ONE 17 (3) (2022) e0264969, https://doi.org/10.1371/journal.pone.0264969.
[44] Y. Demir, H. Şenol, O. Uluçay, Ş. Ateşoğlu, F.S. Tokalı, Morpholine-modified thiosemicarbazones and thiazolidin-4-ones against Alzheimer's key enzymes: from synthesis to inhibition, Comput. Biol. Chem. 120 (2026) 108683, https://doi.org/10.1016/j.compbiolchem.2025.108683.
[45] F.S. Tokalı, H. Şenol, Ş. Ateşoğlu, F. Çakır, P. Tokalı, F. Akbaş, Design and synthesis of new thienopyrimidine derivatives as potential anticancer agents: from cytotoxicity screening to VEGFR inhibition modeling, J. Mol. Struct. 1352 (2026) 144425, https://doi.org/10.1016/j.molstruc.2025.144425.
[46] P. Tokalı, Y. Demir, F. Çakır, H. Şenol, F.S. Tokalı, Design, synthesis, and aldose reductase inhibition assessment of novel quinazolin-4(3H)-one derivatives with 4-bromo-2-fluorobenzene functionality, Bioorg. Chem. 162 (2025) 108614, https://doi.org/10.1016/j.bioorg.2025.108614.
[47] G. Toraman, H. Senol, S.Y. Tütünis, N.R. Tan, G. Topçu, Phytochemical analysis and molecular docking studies of two endemic varieties of Salvia sericeotomentosa, Turk. J. Chem. 47 (5) (2023) 1260–1270, https://doi.org/10.55730/1300-0527.3610.
[48] J. Hou, H. Gong, Z. Gong, X. Tan, X. Qin, J. Nie, H. Zhu, S. Zhong, Structural characterization and anti-inflammatory activities of a purified polysaccharide from fruits remnants of Alpinia zerumbet (Pers.) Burtt. Et Smith, Int. J. Biol. Macromol. 267 (2024) 131534, https://doi.org/10.1016/j.ijbiomac.2024.131534.
[49] I. Toptanci, O. Ketenoglu, M. Kiralan, Assessment of the migration of perfluorinated compounds and primary aromatic amines from PTFE-coated non-stick cookware marketed in Turkey, Environ. Sci. Pollut. Res. 29 (25) (2022) 38535–38549, https://doi.org/10.1007/s11356-022-18783-1.
[50] I. Toptanci, M. Kiralan, O. Ketenoglu, M.F. Ramadan, Monitoring of bisphenol A diglycidyl ether (BADGE) and some derivatives in fish products in the Turkey market, Environ. Sci. Pollut. Res. 29 (35) (2022) 52788–52795, https://doi.org/10.1007/s11356-022-19587-z.
[51] M. Kiralan, I. Toptanci, S. Kiralan, O. Ketenoglu, Monitoring of various contaminants in takeaway articles made from paper and board food contact materials in Turkey, Food Addit. Contam. Part A 42 (7) (2025) 980–989, https://doi.org/10.1080/19440049.2025.2518290.
[52] E. Ören, S. Tuncay, Y.E. Toprak, M. Fırat, İ. Toptancı, F. Karasakal Ö, M. Işık, M. Karahan, Antioxidant, antidiabetic effects and polyphenolic contents of propolis from Siirt, Turkey, Food Sci. Nutr. 12 (4) (2024) 2772–2782, https://doi.org/10.1002/fsn3.3958.
[53] S.Y. Begum, P. Mohamed Imran, A. Kubaib, M.T. Yassin, K. Maniah, Targeted design and synthesis of phenyl-substituted isonicotinyl derivatives with a focus on antimicrobial, antioxidant and antidiabetic properties, J. Mol. Struct. 1320 (2025) 139571, https://doi.org/10.1016/j.molstruc.2024.139571.
[54] H. Karagecili, M.A. Yılmaz, A. Ertürk, H. Kiziltas, L. Güven, S.H. Alwasel, İ. Gulcin, Comprehensive metabolite profiling of Berdav Propolis using LC-MS/MS: determination of antioxidant, anticholinergic, antiglaucoma, and antidiabetic effects, Molecules 28 (4) (2023) 1739, https://doi.org/10.3390/molecules28041739.
[55] I. Gülçin, M. Oktay, E. Köksal, H. Serbetci, S. Beydemir, Ö. Küfrevioglu, Antioxidant and radical scavenging activities of uric acid, Asian J. Chem. 20 (3) (2008) 2079–2090.
[56] M. Isik, E. Dikici, S. Altin, C. Alp, K.K. Kirboga, E. Köksal, S. Beydemir, Phenolic content, antioxidant capacity, and therapeutic potential of Mango (Mangifera indica L.) leaves, Food Sci. Nutr. 13 (5) (2025) e70263, https://doi.org/10.1002/fsn3.70263.
[57] F.S. Tokalı, Y. Demir, Ş. Ateşoğlu, P. Tokalı, H. Şenol, Development of phenolic Mannich bases as α-glucosidase and aldose reductase inhibitors: *in vitro* and in silico approaches for managing diabetes mellitus and its complications, Bioorg. Med. Chem. 128 (2025) 118264, https://doi.org/10.1016/j.bmc.2025.118264.

[58] I. Mamedov, H. Şenol, F. Naghiyev, V. Khrustalev, N. Sadeghian, P. Taslimi, New tetrahydro-isoquinoline derivatives as cholinesterase and α-glycosidase inhibitors: synthesis, characterization, molecular docking & dynamics, ADME prediction, *in vitro* cytotoxicity and enzyme inhibition studies, J. Mol. Liq. 404 (2024) 125006, https://doi.org/10.1016/j.molliq.2024.125006.

[59] F.S. Tokalı, H. Şenol, Ş. Ateşoğlu, P. Tokalı, F. Akbaş, Exploring highly selective polymethoxy fenamate isosteres as novel anti-prostate cancer agents: synthesis, biological activity, molecular docking, molecular dynamics, and ADME studies, J. Mol. Struct. 1319 (2025) 139519, https://doi.org/10.1016/j.molstruc.2024.139519.

[60] A. Farzaliyeva, H. Şenol, P. Taslimi, F. Çakır, V. Farzaliyev, N. Sadeghian, I. Mamedov, A. Sujayev, A. Maharramov, S. Alwasel, İ. Gulçin, Synthesis and biological studies of acetophenone-based novel chalcone, semicarbazone, thiosemicarbazone and indolone derivatives: structure-activity relationship, molecular docking, molecular dynamics, and kinetic studies, J. Mol. Struct. 1321 (2025) 140197, https://doi.org/10.1016/j.molstruc.2024.140197.

[61] B. Zengin Kurt, M. Gökçe, H. Şenol, D. Öztürk Civelek, G. Dandin, I. Gazioglu, Synthesis, cytotoxic evaluation, and in silico studies of novel benzenesulfonamide-thiazolidinone derivatives against colorectal carcinoma, J. Mol. Struct. 1321 (2025) 140153, https://doi.org/10.1016/j.molstruc.2024.140153.

[62] J. Xiang, J. Zhang, Y. Zhao, F.-X. Wu, M. Li, Biomedical data, computational methods and tools for evaluating disease–disease associations, Br. Bioinform. 23 (2) (2022) bbac006, https://doi.org/10.1093/bib/bbac006.

[63] M. Moussaoui, S. Baammi, H. Soufi, M. Baassi, A. El Allali, M.E. Belghiti, R. Daoud, S. Belaaouad, QSAR, ADMET, molecular docking, and dynamics studies of 1,2,4-triazine-3(2H)-one derivatives as tubulin inhibitors for breast cancer therapy, Sci. Rep. 14 (1) (2024) 16418, https://doi.org/10.1038/s41598-024-66877-2.

[64] Z. Köksal, P. Güller, A. Keskin, Lactoperoxidase inhibition by some carnosol and carnosic acid derivatives: *in vitro*, in silico and statistical approaches, Food Biosci. 62 (2024) 105485, https://doi.org/10.1016/j.fbio.2024.105485.